J. Fluid Mech. (1973), *vol.* 61, *part* 2, *pp.* 275–287
Printed in Great Britain

Wind-induced turbulent entrainment across a stable density interface

By JIN WU

Hydronautics, Incorporated, Laurel, Maryland

(Received 14 May 1973)

Turbulent entrainment across a density interface is studied in a laboratory wind–wave tank in which a stably stratified system consisting of two homogeneous fluid layers is introduced. The results indicate that the rate of change of the potential energy of the mixing layer is proportional to the rate of work done by the wind. However, only a very small fraction of the work done by the wind is used for interfacial mixing or developing a seasonal thermocline. A formula relating the entrainment rate to the density stratification and the wind-friction velocity is derived from the experimental results.

1. Introduction

The simplest condition for studying vertical mixing in a stably stratified fluid is the case of a density interface. Experiments with relative motion between a fresh-water and a salt-water layer were conducted by Ellison & Turner (1959). The ratio between the entrainment velocity and the mean-flow velocity was found to be a function of the Richardson number defined in terms of the density difference between the two fluids and the depth and mean velocity of the moving fluid. A further and more detailed investigation of entrainment processes in steady-state shearing flows of stratified fluids was reported by Moore & Long (1971). Experiments on turbulent entrainment induced by an oscillating grid without mean flow were performed by Rouse & Dodu (1955) and Turner (1968). It was suggested in the former study and verified partially in the latter study that the rate of change of potential energy of the stratified fluid is proportional to the rate of work done by the mechanical stirrer.

Turner's (1968) experiments were conducted in connexion with the study of thermocline erosion (Phillips 1966). Pursuing the same line, Kato & Phillips (1969) and Moore & Long (1971) conducted their experiments on the penetration of a turbulent layer into a continuously stratified fluid in an annular tank. The turbulence was produced by shear, induced either by rotating the tank cover or by ejecting and withdrawing fluid. The modelling of oceanic entrainment at the seasonal thermocline is conducted here by performing experiments in a stratified wind–wave tank with direct wind mixing. The results provide direct experimental demonstrations that a surface layer penetrates into a heavier uniform layer at a constant rate, and that only a small portion of the work done by the wind is used for mixing.

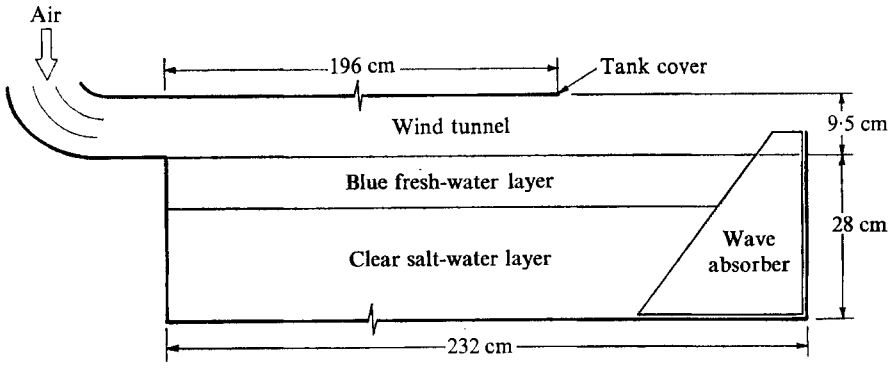

FIGURE 1. General arrangement.

2. Equipment and experiment

2.1. *Wind-friction velocity and surface-drift current*

The experiment was conducted in a transparent wind–wave tank 20·5 cm wide and 232 cm long; the tank was covered for the first 196 cm (see figure 1). A blower was installed at the upstream end of the tank and a permeable-type wave absorber at the downstream end. The maximum operable wind velocity is 15 m/s within a 9·5 cm deep wind tunnel over 28 cm deep water.

The wind boundary layer was surveyed with a Pitot-static tube at five sections nearly equally spaced along the tank. The velocity profiles near the water surface were found to follow the logarithmic law, the Kármán–Prandtl velocity distribution (Schlichting 1968, chap. 19); the friction velocity u_* of the wind was then determined from the logarithmic profile $u_* = (\tau/\rho_a)^{\frac{1}{2}}$, where τ is the wind stress and ρ_a is the density of air. For each fetch, the friction velocities were first plotted versus the wind velocities; a smooth curve was then fitted through the data to obtain the friction velocity at every integral wind velocity (1, 2, 3 m/s, etc.). Subsequently, for each integral wind velocity, the friction velocities obtained from different fetches were plotted, and a curve was fitted through the data and extended to both ends of the tank. Finally, the area under the curve was integrated to find the average wind-friction velocity $\overline{u}_{*a}$, see figure 2 (*a*). The variation of the friction velocity along the tank was generally less than $\pm$ 20 % of the mean value. From the friction velocity and the surface roughness (also obtained from the wind profile), the wind boundary layer was found to be hydrodynamically rough when the wind velocity was greater than 3 m/s. The wind-mixing experiments reported herein were conducted in the hydrodynamically rough flow regime.

The surface-drift current W_s was measured by timing small floats passing two stations at a fixed distance apart along the tank. Spherical particles about 1·5 mm in diameter having a specific gravity of 0·95 were used as surface floats. Because a steep current gradient exists near the water surface, the velocity indicated by a float of such a size may be slightly lower than the actual surface drift (Wu 1968). However, it will become clear later that we need the surface-drift current here

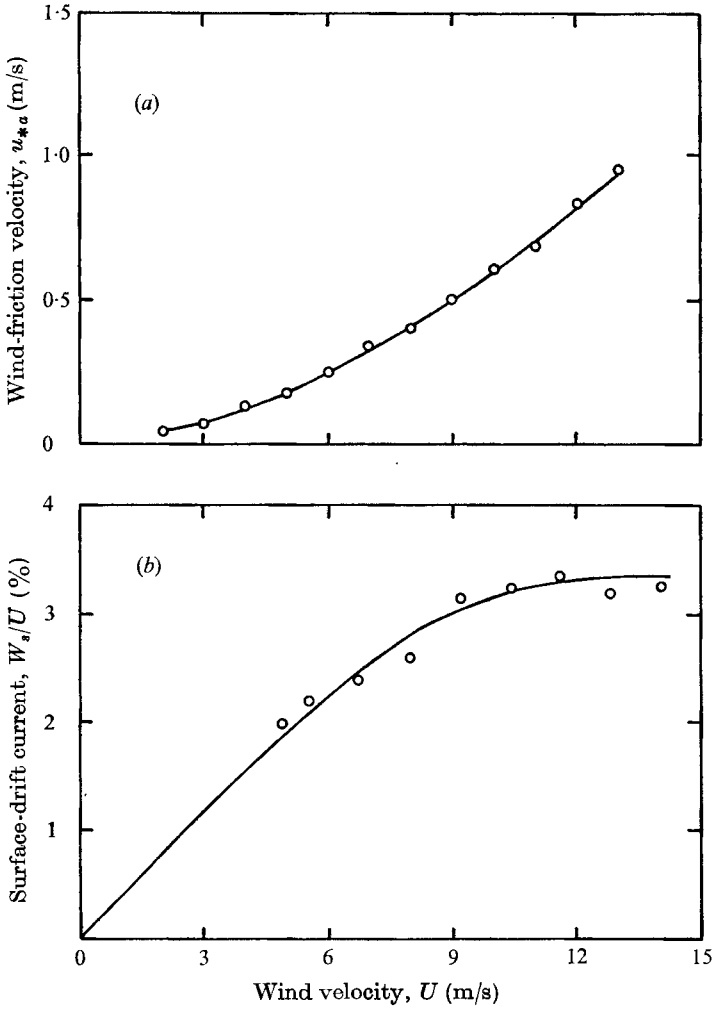

FIGURE 2. (*a*) Wind-friction velocities and (*b*) surface-drift currents under various wind conditions. The wind velocity U is measured at $\frac{2}{3}$ of the tunnel height above the water surface; at this reference elevation the maximum wind velocity within the tunnel is generally measured.

only for a qualitative comparison. The ratio between the surface-drift current and the wind velocity U is plotted in figure 2(*b*), where each data point was averaged from more than 10 readings.

2.2. *Stratified fluids*

As shown in figure 1, the experiments were conducted in a stratified system with two layers of fluids, blue-coloured fresh water lying over clear salt water of various densities. The initial thickness of the upper layer was always kept at 10 cm. The salt water was introduced into the tank first, and the fresh water carefully introduced through a floating diffuser immediately before the experiment to assure a sharp density interface.

2.3. *Experiment*

The wind velocity at the reference height in the tank was continuously monitored during the test with a Pitot-static tube and a pressure transducer unit. The gate which controlled the wind velocity was opened very slowly so that the desired wind velocity was reached in a period of about three minutes. Such a procedure is necessary in order to avoid an impulsive start, which would introduce excessive disturbance in the fluid. The downward penetration of the blue layer under a steady wind was photographed with a movie camera. Some sample pictures are shown in figure 3 (plate 1).

In the present experiment, the molecular diffusion at the stable density interface is negligible in comparison with the turbulent diffusion. The molecular diffusivity of salt in water is of the order of 10^{-5} cm^2/s, while the present measured diffusivity even for the slowest case is of the order of 10^{-2} cm^2/s. Rather violent turbulent motion was clearly visible within the upper layer with the aid of small foreign particles which were always present. The lower layer was stationary with no visible motion. The density interface was wavy and rough, with high frequency disturbances superimposed on short-crested irregular waves. The interface was also observed to be bombarded by low frequency vortices, appearing as blue puffs which penetrated deeply into the clear layer and then retreated. Wisps of fluid often developed during penetration and were detached from the crests of disturbances in the manner observed and visualized by Moore & Long (1971). The blue layer, always homogeneous in colour, undoubtedly marked the turbulent mixing zone with a rather sharp density jump at its lower boundary.

As shown in figure 3, there was only a very slight tilt at the density interface, because an appreciable density jump always existed at the interface. Observations showed a wind-induced drift (downwind) current near the free surface and a very weak and highly irregular return (upwind) flow near and above the density interface. The irregularity of the return flow apparently results from superimposing a very weak current on a highly turbulent flow. The fact that this weak current, producing negligible entrainment at the interface, actually smoothed the irregularities in the mixing system in the present tank due to longitudinal variations of the wind-friction velocity will be discussed later.

3. Previous and present experiments

3.1. *Experiments with grid stirring*

As in an earlier experiment of Rouse & Dodu (1955), tests using a stirring grid were carried out by Turner (1968) to study turbulent entrainment across a density interface between two liquids, the lighter liquid occupying the upper layer. The low Reynolds number turbulence in Turner's experiment was produced by stir ring at a fixed distance from the interface, as the fluid in the lower layer was continuously withdrawn from the bottom of the tank during the stirring at such a rate to compensate exactly for the entrainment (upward movement of the interface).

An 'overall Richardson number' R_i was defined as

$$R_i = g\frac{\Delta\rho}{\rho}\frac{1}{ln^2}, \tag{1}$$

in which g is the gravitational acceleration, $\Delta\rho/\rho$ is the dimensionless density difference at the interface, l is a length scale considered to be constant throughout the experiment by using the same grid at a fixed distance from the interface, and n is the frequency of the stirring grid and is considered to specify the velocity scale for his experiment with a fixed geometry. The entrainment velocity u_e, the rate of displacement of the interface, was shown to follow roughly

$$u_e/n \sim R_i^{-1} \tag{2}$$

for tests with density differences produced by heat alone, and for tests with salinity differences at low values of R_i. The entrainment rate was found to fall off progressively with increasing R_i in the salinity experiments, and approached the form $u_e \sim R_i^{-\frac{3}{2}}$. One of the consequences of (2) is that the rate of change of potential energy of the stirred layer is proportional to the rate of production of turbulent energy by the grid, as was first pointed out by Rouse & Dodu (1955).

3.2. *Experiments with constant shear*

Kato & Phillips (1969) conducted their experiment in an annular tank with a rotating top to apply constant stress to the surface of initially quiescent fluid with a uniform density gradient. The surface stress was applied by a plastic screen hung from the top of the tank, and was determined by measuring the total torque of the wheel which supported the top of the tank. Later, experiments were performed by Moore & Long (1971) in a similar tank but with shear produced by ejecting fluid into, and withdrawing fluid from, the tank.

The entrainment velocity of the mixing layer penetrating into the lower stratified fluid was found to be

$$\frac{u_e}{u_*} = 2{\cdot}5\frac{\rho u_*^2}{g\Delta\rho H}, \quad \Delta\rho = \left(\frac{\partial\rho}{\partial z}\right)_0\frac{H}{2}, \tag{3}$$

in which u_* is the friction velocity, H is the depth of the mixed fluid and $(\partial\rho/\partial z)_0$ is the initial density gradient of the stratified fluid. The right-hand side of (3) is also of the form R_i^{-1}.

3.3. *Present experiment with wind mixing*

As pointed out by Turner (1968) and Kato & Phillips (1969), the experiments with an oscillating grid retain an inherent difficulty in defining the structure and scale of turbulence generated by mechanical agitation. Moving towards simulating more realistic thermocline erosion, Kato & Phillips generated the turbulent layer in an annular tank by applying a known horizontal stress at the upper surface of a stratified fluid. Carrying the simulation a step further, the present experiment has been conducted in a wind–wave tank, where a wind blowing over a wavy water surface provided a truly wind-excited upper turbulent layer. In this case, the horizontal stress at the upper surface is not only given but also

is directly produced by a turbulent wind, unlike earlier experiments in which the turbulence may depend on the special mechanical method of generation.

Secondary flow undoubtedly existed in the present tank as well as in the tanks used by Kato & Phillips (1969) and by Moore & Long (1971). The secondary flow was produced by the centrifugal force in the latter tanks, and the interface tilted radially. For the present tank, the flow near the density interface was induced by the wind stress, and the interface tilted longitudinally. The distribution of the downwind drift and the upwind return currents in a wind–wave tank was measured by Baines & Knapp (1965). They found that the maximum return current is about three times the friction velocity u_* of the drift current. The latter was obtained by assuming stress continuity across the air–water interface, or

$$\rho_a \bar{u}_{*a}^2 = \rho u_*'^2, \tag{4}$$

where ρ_a and ρ are the densities of air and water, respectively; u_*', the friction velocity in water according to (4), as will be discussed later, provides an overestimate of the true friction velocity u_* of the drift current.

Following Ellison & Turner (1959), the Richardson number governing the interfacial mixing due to a mean current is defined as

$$R_i = g\Delta\rho D/\rho u_*^2, \tag{5}$$

where D is the depth of the moving layer. In the present case, the upwind current near the density interface extends about halfway down through the mixing layer. Taking half the depth as D and using u_*' for u_*, the Richardson number in the present experiment was found to be always far greater than 0·8. Therefore, the return current should not introduce any significant interfacial entrainment. On the other hand, the circulation set up by the downwind surface drift and the upwind bottom current in the mixing layer should serve the purpose of smoothing the mixing system. The latter consisted of slightly different local mixing as a result of the longitudinal variation of the wind shear. In other words, the bottom current in the mixing layer helps to move the excessively entrained fluid from high to low shear zones.

For a linearly stratified fluid such as that in the experiments of Kato & Phillips and of Moore & Long, when the interface penetrates deeper, the effects of wind mixing at the interface decrease while the density difference across the interface increases. Consequently, as indicated in (2) and (3), the rate of thickening of the mixing layer decreases drastically with time, causing inaccuracy in measurements. A stably stratified system consisting of two layers, a lighter layer above a heavier layer, is adopted for the present experiment. In this case, as the mixing layer deepens, both the density difference across the interface and the effects of wind mixing at the interface decrease. According to previous results, equations (3), a constant rate of entrainment is expected.

4. Results and discussion

4.1. *Energy balance*

The mean elevation of the lower boundary of the mixing layer, traced from the film, is plotted versus the time in figure 4. The elevation $H - H_0$ is the distance

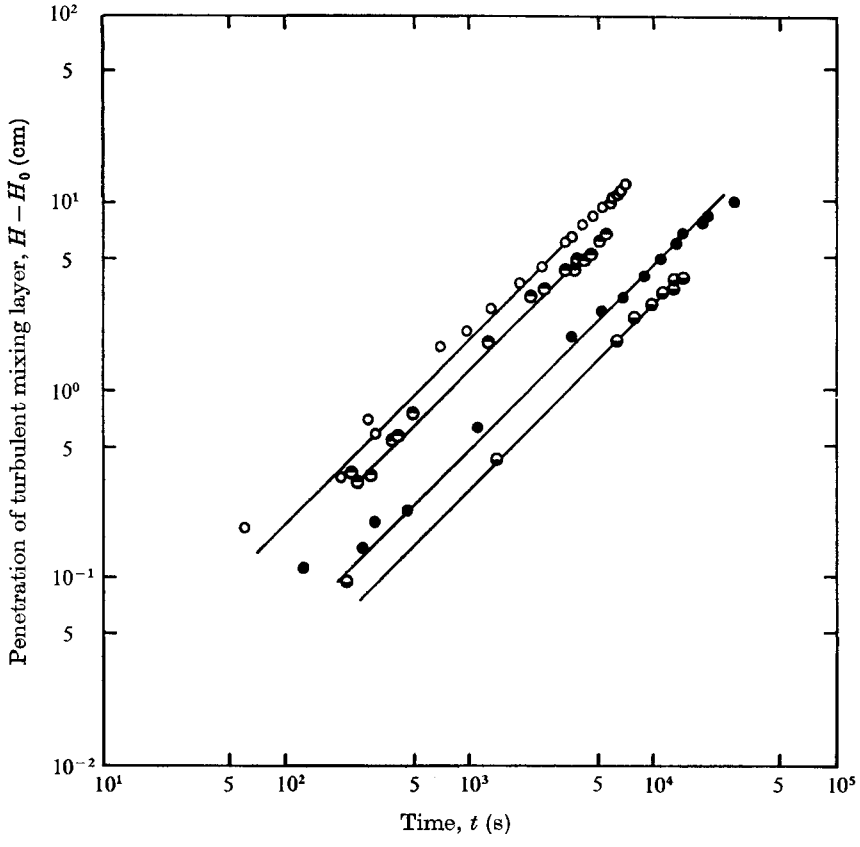

FIGURE 4. Deepening of turbulent mixing layer. ○, $(\Delta\rho/\rho)_0 = 2\,\%$; $\overline{u}_{*a} = 49{\cdot}0$ cm/s; ◓, $(\Delta\rho/\rho)_0 = 4\,\%$, $\overline{u}_{*a} = 53{\cdot}1$ cm/s; ●, $(\Delta\rho/\rho)_0 = 8\,\%$, $\overline{u}_{*a} = 50{\cdot}3$ cm/s; ◒, $(\Delta\rho/\rho)_0 = 16\,\%$, $\overline{u}_{*a} = 53{\cdot}2$ cm/s.

measured from the initial lower boundary of the blue (fresh-water) layer and t is the time after the wind reached a constant velocity. It is seen that for all four runs, with various density differences at the interface, the distance of penetration varies linearly with time; a straight line with a slope of unity is seen in figure 4 to fit fairly well through each set of data. The velocity of penetration of the mixing layer is therefore constant throughout each test.

An idealized picture of the change in the density distribution of the stratified fluid in the present tank due to wind mixing is shown in figure 5, where the mixing layer is seen to be deepened by ΔH in a period of Δt. If we designate, at time t, ρ as the density of the mixed fluid and $\Delta\rho$ as the density difference at the interface, the rate of change $\Delta E_p/\Delta t$ of potential energy per unit surface area can be written as

$$\frac{\Delta E_p}{\Delta t} = \frac{1}{\Delta t}\left[\left(\frac{\Delta H \Delta\rho}{H}\right) g\,(H+\Delta H)\left(\frac{H+\Delta H}{2}\right)\right]. \tag{6}$$

Neglecting the higher order terms, we have

$$\Delta E_p/\Delta t = \tfrac{1}{2} H \Delta\rho g \Delta H/\Delta t. \tag{7}$$

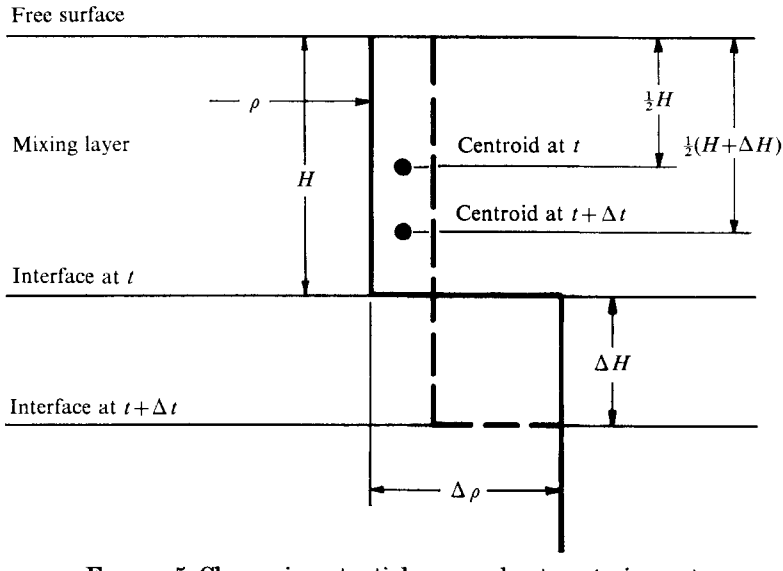

FIGURE 5. Change in potential energy due to entrainment.

As discussed earlier, the density difference $\Delta\rho$ at the interface is inversely proportional to the distance of penetration H: $H\Delta\rho$ = constant. The rate of entrainment $\Delta H/\Delta t$ is seen in figure 4 to be constant. Consequently, the right side of (7) is constant and the potential energy of the mixing layer, therefore, increases linearly with time. Since the rate of work done by the wind, or the wind velocity, remains constant for each run, the rate of change of the potential energy of the mixing layer is therefore proportional to the rate of work done by the wind. This is the energy balance first suggested by Rouse & Dodu (1955) and verified later under different conditions by Turner (1968), Kato & Phillips (1969) and Moore & Long (1971). However, the present results represent a more direct proof of this balance with a wind-mixing system.

4.2. *Wind mixing*

The rate $\Delta E_k/\Delta t$ of work done by the wind stress per unit surface area is generally expressed (Kraus & Turner 1967) as

$$\Delta E_k/\Delta t = \tau W_s = \rho_a \overline{u}_{*a}^2 W_s, \tag{8}$$

where, as defined earlier, τ is the wind stress and W_s is the surface-drift current.

By comparing the rate of increase of the potential energy of the mixing layer due to entrainment and the rate of work done by the wind stress, we can determine the fraction of the work done by the wind used for mixing at the density interface, or for developing the seasonal thermocline. From (7) and (8), we have

$$\frac{\Delta E_p}{\Delta E_k} = \frac{1}{2}\frac{\Delta\rho g H \Delta H/\Delta T}{\rho_a \overline{u}_{*a}^2 W_s}. \tag{9}$$

The ratio for the various tests is tabulated in table 1. The values shown here indicate that the wind momentum is consumed almost entirely by generating

$(\Delta\rho/\rho)_0$	0·02	0·04	0·08	0·16
$\Delta E_p/\Delta E_k$	0·0024	0·0025	0·0022	0·0023

TABLE 1. Energy consumed on entrainment

surface waves and producing drift currents. A surprisingly small fraction, about $\frac{1}{4}$%, of the work done by the wind is used for developing the seasonal thermocline.

4.3. *Empirical formula*

The rate of entrainment is usually related to the Richardson number R_i, which in the present case can be defined as

$$R_i = g\Delta\rho H/\rho_a \overline{u}_{*a}^2. \tag{10}$$

It is noted that, instead of the density and friction velocity of water, the density and friction velocity of air are used here, because $\overline{u}_{*a}$ is directly measured in the present experiment and u_* is unknown. If we assume continuity of the shear stress across the interface, R_i will have the same value for both cases. The term $H\Delta\rho$, as discussed earlier, was kept constant throughout each test, or

$$H\Delta\rho = H_0(\Delta\rho)_0,$$

where $(\Delta\rho)_0$ is the initial density difference across the interface. The entrainment velocity, deduced from figure 4, is plotted versus the initial Richardson number in figure 6. The straight line with a slope of -1 fitted through the data can be expressed as

$$u_e/\overline{u}_{*a} = 0{\cdot}0026\rho_a \overline{u}_{*a}^2/g(\Delta\rho)_0 H_0. \tag{11}$$

4.4. *Wave drag and comparison of results*

As was first suggested by Stewart (1961), an appreciable portion of the drag exerted by the water surface on the wind is in the form of wave drag. Pursuing another line, the wind stress was shown (Wu 1970) to be supported by the form drag on roughness elements (small waves). As was pointed out by Lighthill (1971), this horizontal pressure force cannot excite a horizontal current directly, but excites wave trains carrying the transferred momentum. In other words, as he stated, the momentum transferred by the wind stress goes principally into the waves.

In order to estimate the wave drag in the present tank, we assume that the wave momentum M per unit area of the water surface can be approximated by the following expression for irrotational waves:

$$M = \frac{E}{c} = \frac{\frac{1}{8}\rho g\overline{h}^2}{(g\overline{\lambda}/2\pi)^{\frac{1}{2}}}, \tag{12}$$

where E is the wave energy per unit surface area, $\overline{h}$ and $\overline{\lambda}$ are the average height and length of waves, respectively, and c is the phase velocity calculated from $\overline{\lambda}$ as shown. Long after the onset of the wind, the waves reach an equilibrium state

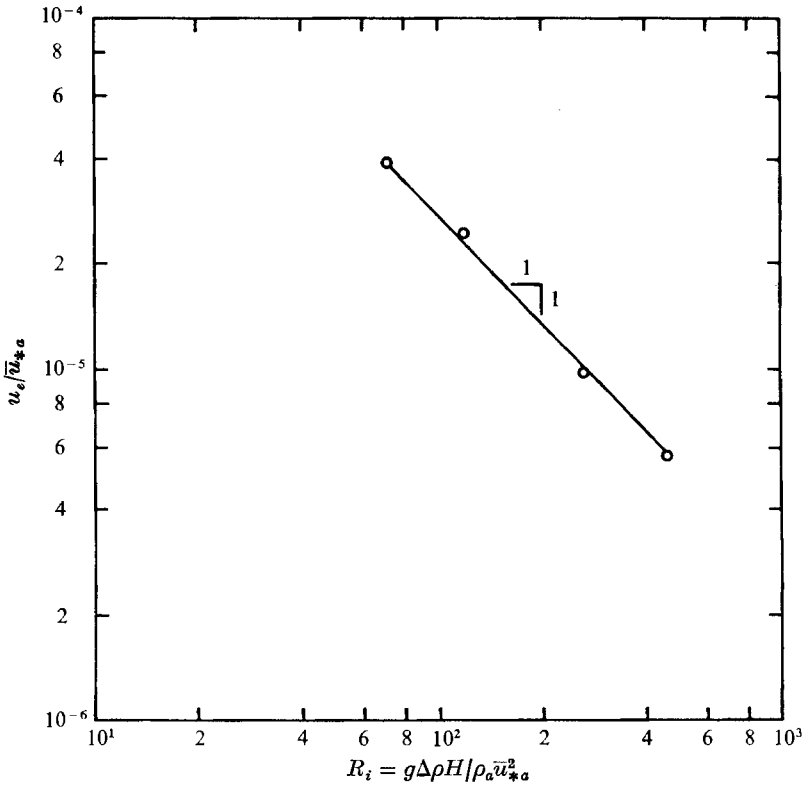

FIGURE 6. Variation of entrainment rate with Richardson number R_i.

locally; the rate of increase of wave momentum in the wind direction can be considered as the wave drag. The coefficient C_w, of wave drag, can therefore be estimated from

$$C_w = c\frac{dM}{dx}\Big/\rho_a U^2 = \tfrac{3}{16}\rho g\bar{h}\frac{d\bar{h}}{dx}\Big/\rho_a U^2, \tag{13}$$

with an additional approximation $d\bar{\lambda}/dx = (\bar{\lambda}/\bar{h})\,d\bar{h}/dx$, where x is the axis along the direction of the wind.

From wave records, the average wave heights near the downstream end of the tank, no less than three wavelengths upstream from the wave absorber, were obtained at various wind velocities. For a rough estimation, we further consider $d\bar{h}/dx = \bar{h}/L$, where L is the fetch of the wave-measuring station; the results are shown in figure 7. The wind-mixing experiments were conducted at a wind velocity of about 9 m/s, at which the wave-drag coefficient is about 0·0017, in comparison with the wind-stress coefficient 0·0032. Therefore, in the present tank the ratio τ_w/τ is about 0·53, falling between the values 0·2 obtained by Stewart (1961) and 0·8 obtained by Dobson (1971).

Accepting the value 0·53, we can find the ratio between the actual friction velocity in water u_* and the value calculated from the stress continuity as $u_*/u'_* = (1-0{\cdot}53)^{\frac{1}{2}} = 0{\cdot}685$, and rewrite (11) as

$$\frac{u_e}{u_*} = 0{\cdot}234\frac{u_*^2}{g(\Delta\rho/\rho)_0 H_0}. \tag{14}$$

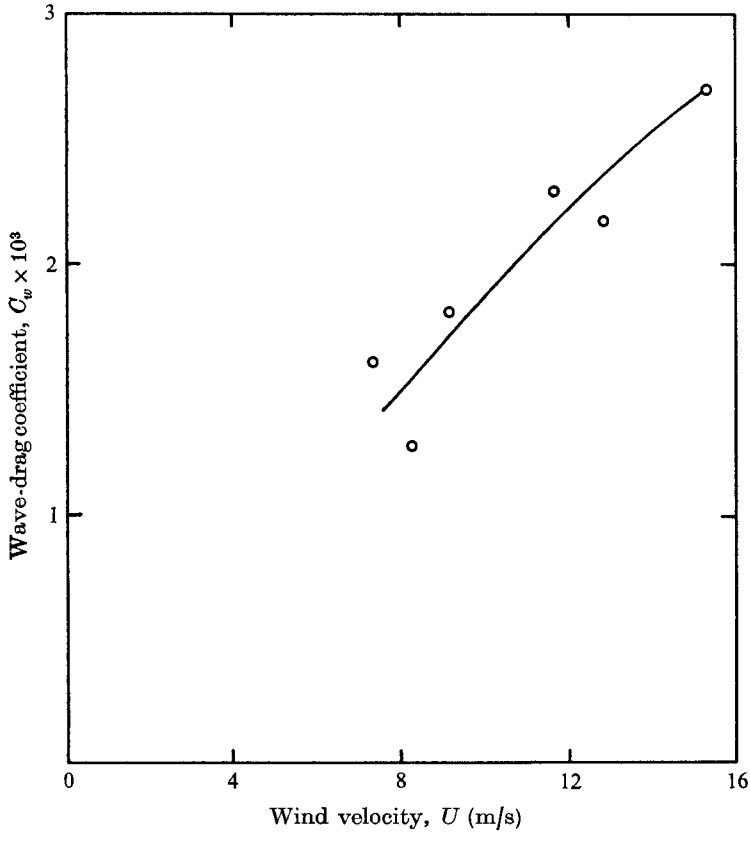

FIGURE 7. Wave-drag coefficients at various wind velocities.

The present coefficient 0·234 is much smaller than the coefficient 2·5 obtained by Kato & Phillips (1969). The discrepancy is probably due to different distributions of currents near the density interface, as pointed out by Professor O. M. Phillips (private communication). The current in the annular tank used by Kato & Phillips decreased monotonically from the tank cover towards the density interface and approached zero asymptotically at the interface. The current distribution in the present tank between the free surface and the density interface should be very similar to that measured by Baines & Knapp (1965) in their wind–wave tank. They reported that the current decreased rapidly near the free surface, as in Kato & Phillips's case, and crossed zero at about two-thirds of the water depth from the free surface. The current for the lower third of the water depth was in the opposite direction to the wind.

4.5. *Seasonal-thermocline model*

Substituting (11) into (7), we have

$$\Delta E_p/\Delta t = 0{\cdot}0013\rho_a \overline{u}_{*a}^3 = 0{\cdot}0374\tau u'_*. \tag{15}$$

The results obtained in the previous subsection indicate that the wind stress τ_c supported by currents is about 0·47 of the total wind stress, and that the fric-

tion velocity of the current is about 0·685 of the value calculated from stress continuity. If these results are accepted (15) becomes

$$\Delta E_p/\Delta t = 0{\cdot}116\tau_c u_*. \tag{16}$$

A one-dimensional model of the seasonal thermocline was proposed by Kraus & Turner (1967). They suggested on dimensional grounds that the total rate of work done by the wind is $\tau u'_*$. The partitioning of the wind stress between wave- and current-supported components was not considered by them. Taking into consideration the wave drag, this rate of working by the wind should be expressed as $\tau_c u_*$. Compared with (16), we see again that only a small portion of this rate of working is used for erosion of the seasonal thermocline.

5. Conclusion

Turbulent entrainment across a density interface between two fluids, the lighter being above the heavier, was studied with mixing directly induced by the wind. The rate of entrainment was found to be constant. An empirical formula relating the entrainment rate to the mixing-layer thickness, the density difference and the wind-friction velocity has been derived. Qualitatively, the present results compare favourably with other laboratory results of interfacial mixing with turbulence generated by mechanical stirring. However, a much slower rate of entrainment is obtained in the present experiment than was obtained by Kato & Phillips. This is probably due to a different distribution of currents near the density interface; further studies are definitely required to clarify this point. It has also been illustrated that the change of potential energy of the mixing layer due to entrainment is proportional to the rate of work done by the wind on interfacial mixing. However, a very small fraction of the work done by the wind was found to be actually used for interfacial mixing.

I am very grateful to Professor O. M. Phillips for many valuable suggestions and helpful discussions and reviewing of this manuscript. This work was part of a research programme on air–sea interactions under the direction of Dr S. G. Reed.

REFERENCES

Baines, W. D. & Knapp, D. J. 1965 Wind driven water currents. *J. Hydraul. Div. A.S.C.E.* **91**, 205–221.

Dobson, F. W. 1971 Measurements of atmospheric pressure on wind-generated sea waves. *J. Fluid Mech.* **48**, 91–127.

Ellison, T. H. & Turner, J. S. 1959 Turbulent entrainment in stratified flows. *J. Fluid Mech.* **6**, 423–448.

Kato, H. & Phillips, O. M. 1969 On the penetration of a turbulent layer into stratified fluid. *J. Fluid Mech.* **37**, 643–655.

Kraus, E. B. & Turner, J. S. 1967 A one-dimensional model of the seasonal thermocline, II. The general theory and its consequences. *Tellus*, **19**, 98–106.

Lighthill, M. J. 1971 Time-varying currents. *Phil. Trans. Roy. Soc.* A **270**, 371–390.

Moore, M. J. & Long, R. R. 1971 An experimental investigation of turbulent stratified shearing flow. *J. Fluid Mech.* **49**, 635–655.

PHILLIPS, O. M. 1966 *The Dynamics of the Upper Ocean.* Cambridge University Press.

ROUSE, H. & DODU, J. 1955 Diffusion turbulente à traverse une discontinuité de densité. *Houille Blanche*, **10**, 522–532.

SCHLICHTING, H. 1968 *Boundary Layer Theory.* McGraw-Hill.

STEWART, R. W. 1961 The wave drag of wind over water. *J. Fluid Mech.* **10**, 189–194.

TURNER, J. S. 1968 The influence of molecular diffusivity on turbulent entrainment across a density interface. *J. Fluid Mech.* **33**, 639–656.

WU, J. 1968 Laboratory study of wind-wave interactions. *J. Fluid Mech.* **34**, 91–111.

WU, J. 1970 Wind-wave interactions. *Phys. Fluids*, **13**, 1926–1930.

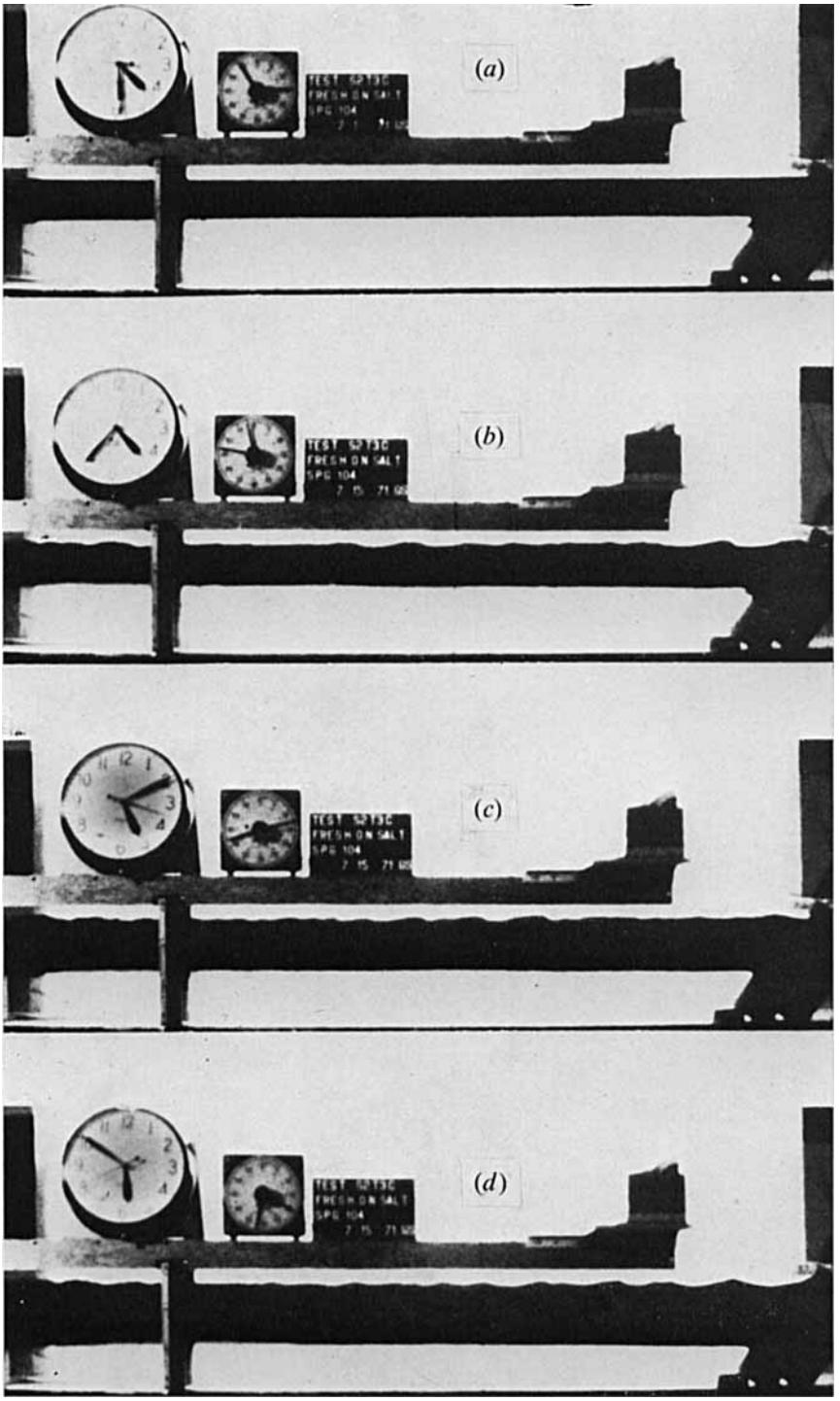

FIGURE 3. Sample pictures. Waves are seen at the free surface and the mixing layer is seen as the dark layer. Picture (*a*) was taken before the test and (*b*), (*c*) and (*d*) illustrate the thickening of the mixing layer.